AIP | Journal of Applied Physics

Structural transitions in [001]/[111]-oriented 0.26Pb(In1/2Nb1/2)O3-0.46Pb(Mg1/3Nb2/3)O3-0.28PbTiO3 single crystals probed via neutron diffraction and electrical characterization

Qian Li, Yun Liu, Jian Wang, Andrew J. Studer, Ray L. Withers et al.

Citation: J. Appl. Phys. **113**, 154104 (2013); doi: 10.1063/1.4802669
View online: http://dx.doi.org/10.1063/1.4802669
View Table of Contents: http://jap.aip.org/resource/1/JAPIAU/v113/i15
Published by the American Institute of Physics.

Structural transitions in [001]/[111]-oriented $0.26Pb(In_{1/2}Nb_{1/2})O_3$-$0.46Pb(Mg_{1/3}Nb_{2/3})O_3$-$0.28PbTiO_3$ single crystals probed via neutron diffraction and electrical characterization

Qian Li,[1] Yun Liu,[1,a)] Jian Wang,[1] Andrew J. Studer,[2] Ray L. Withers,[1] Zhenrong Li,[3] and Zhuo Xu[3]
[1]*Research School of Chemistry, The Australian National University, ACT 0200, Australia*
[2]*Bragg Institute, Australian Nuclear Science and Technology Organisation (ANSTO), NSW 2232, Australia*
[3]*Electronic Materials Research Laboratory (EMRL), Xi'an Jiaotong University, Shaanxi 710049, China*

(Received 18 November 2012; accepted 8 April 2013; published online 19 April 2013)

We report changes in the metric symmetry of unpoled and electrically poled single crystals of $0.26Pb(In_{1/2}Nb_{1/2})O_3$-$0.46Pb(Mg_{1/3}Nb_{2/3})O_3$-$0.28PbTiO_3$, as revealed by neutron diffraction in conjunction with electrical measurements. The unpoled crystals show relaxor characteristics and an average rhombohedral symmetry that persists from ambient temperature up to the Curie temperature of ~165 °C. Poling along a [111] direction enhances the rhombohedral distortion away from cubic metric symmetry but appears not to induce any monoclinic phases. By contrast, the poled [001]-oriented crystal has orthorhombic (or monoclinic M_C) metric symmetry at 25 °C. An intermediate transition to a metrically tetragonal phase around 120 °C is confirmed for both poled crystals. © *2013 AIP Publishing LLC* [http://dx.doi.org/10.1063/1.4802669]

I. INTRODUCTION

Lead-based, relaxor ferroelectric single crystals (RF SCs) are important materials widely utilized in sensors and actuators as a result of their ultra-high piezoelectric properties.[1–3] In general, RF SCs are solid solutions of tetragonal (*T*), ferroelectric $PbTiO_3$ (PT) and pure relaxors that exhibit either rhombohedral (*R*) or pseudo-cubic (*C*) structures, e.g., $Pb(Zn_{1/3}Nb_{2/3})O_3$ (PZN) and $Pb(Mg_{1/3}Nb_{2/3})O_3$ (PMN). The desirable properties of such materials occur within so-called morphotropic phase boundary (MPB) regions. The metrically monoclinic (*M*) phases reported near these MPB regions from diffraction experiments,[4–8] further rationalized by *ab initio* calculations derived from polarization rotation theory,[9] are widely considered to be the origin of the high piezoactivity of RF SCs'. Three distinct types of monoclinic phases have been reported, e.g., M_A and M_C of space group symmetry *Cm*, and *Pm*, respectively. In each of these phases, the polarization vector, $\boldsymbol{P}_s$, is no longer constrained to high symmetry directions, e.g., [111], [001], or [110], as is the case for the *R*, *T*, and *O* (orthorhombic) phases. Instead, it can rotate continuously within a particular lattice plane, defined by the unique monoclinic *b* axis direction. Despite reasonable doubts cast on the existence of such *M* phases,[10,11] the *M* phase standpoint remains self-consistent and effective in linking the effects of external stimuli, including temperature, *E* (electric)-field as well as mechanical stress,[12,13] to the structural response of RF SCs.

Recently, a new ternary RF SC system has been developed by incorporating $Pb(In_{1/2}Nb_{1/2})O_3$ into PMN-PT (that is, PIN-PMN-PT), resulting in a substantial improvement in both temperature and power windows for practical use. Systematic property characterizations have been carried out on PIN-PMN-PT SCs by Zhang *et al.* and other groups,[2,3] mainly from the perspective of potential applications. Detailed structural studies on these RF SC materials, and their behavior under external stimuli, are relatively sparse to date. Given this, we here present an *in situ* neutron diffraction study on near-MPB 0.26PIN-0.46PMN-0.28PT SCs in both [001] and [111] (in pseudo-*C* settings unless subscripted) orientations. Usually, [001]-oriented RF SCs yield both large field-induced strains as well as a giant longitudinal piezoelectric effect, while maximal pyroelectric properties can be detected along the [111] direction.[14] Both orientations are thus of considerable technological importance. In conjunction with electrical measurements, we have therefore investigated the metric symmetry and average structures of PIN-PMN-PT SCs in both unpoled and poled states at several critical temperatures. This provides clear evidence for the various phase transitions undergone by this RF SC material.

II. EXPERIMENTAL

0.26PIN-0.46PMN-0.28PT SCs were grown using the vertical Bridgman technique. Plate samples (~5 × 5 × 0.5 mm) were cut along [001] and [111] directions from positions close by in the boule. Silver electrodes were then fired on the resultant 5 × 5 mm faces, allowing sample poling under a 15 kV/cm *E*-field at 25 °C. The dielectric properties of the crystals were measured in a furnace using an Agilent E4980 *LCR* meter. Pyroelectric currents were recorded with a Keithley 6517 electrometer as the poled crystals were heated at a 2 °C/min rate. The temperature dependent polarization-field (*P*-*E*) and strain-field (*S*-*E*) hysteresis loops of the same samples were also measured using an aixACCT TF2000 system.

Neutron diffraction experiments were performed at the OPAL reactor (ANSTO) using the WOMBAT diffractometer,[15]

a)Author to whom correspondence should be addressed. Electronic mail: yliu@rsc.anu.edu.au.

which features a two-dimensional (2D) curved area detector covering a 120° angular range of 2θ in 0.0625° pixel size steps (Z-axis range $\sim\pm 8°$). Neutron beams with wavelength $\lambda = 1.702$ Å were selected with a Ge(115) monochromator. A resolution of $\triangle d/d \sim 0.005$ was achieved over the studied 2θ range. The samples were placed in a cryo-furnace and mounted on an Eulerian cradle for alignment; the basic protocol was to align the scattering vectors (normal to each selected lattice plane) within the equatorial plane of the diffractometer and scan the corresponding reflections over a 1.5° rocking angle/ω in steps of 0.05°. The crystals were poled *in situ* and the reflections measured in heating runs.

III. RESULTS AND DISCUSSION

Figure 1 shows the measured temperature dependent behavior of the dielectric constant and the associated pyroelectric current of both the poled and unpoled SC samples. All the crystals show a broad peak maximum in the dielectric constant, near $T_{max} \sim 180\,°C$. Poling only induces small shifts in the position of these peaks. Close inspection reveals a clear anomaly at ~165 °C (prior to T_{max}) in the dielectric constant spectrum of the [001] poled crystal. Above this anomaly, the dielectric frequency dispersion becomes noticeably stronger. This dielectric anomaly also correlates with a major peak in the pyroelectric current, and clearly points to the Curie temperature, T_C.[16] A similar T_C anomaly was also found for the [111] poled crystal at a closer-to-T_{max} point, but in common are less evident for the unpoled samples. In addition, a clear shoulder in the dielectric constant spectrum for both poled crystals occurs at 120 °C–125 °C and again correlates well with a peak/s in the respective pyroelectric current curves. By contrast, the dielectric constant spectra of their unpoled counterparts do not show such a shoulder and smoothly increase over this temperature region.

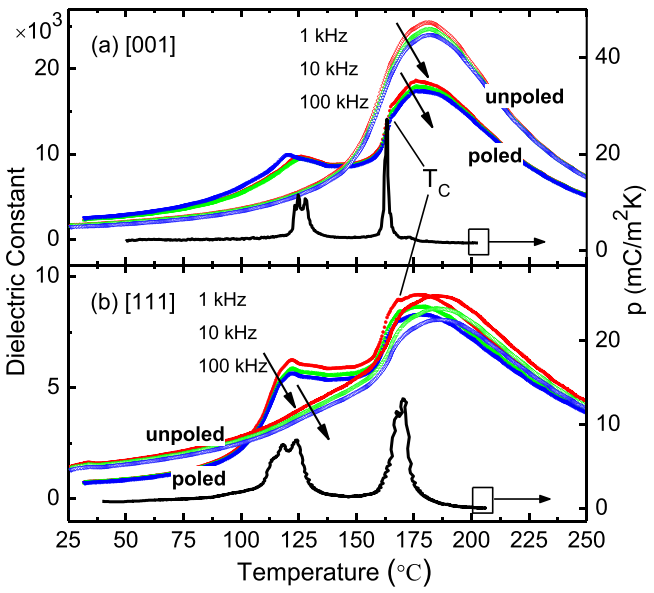

FIG. 1. Temperature dependence of dielectric constant and pyroelectric current (represented in pyroelectric coefficient p) for (a) [001]- and (b) [111]-oriented 0.26PIN-0.46PMN-0.28PT single crystals.

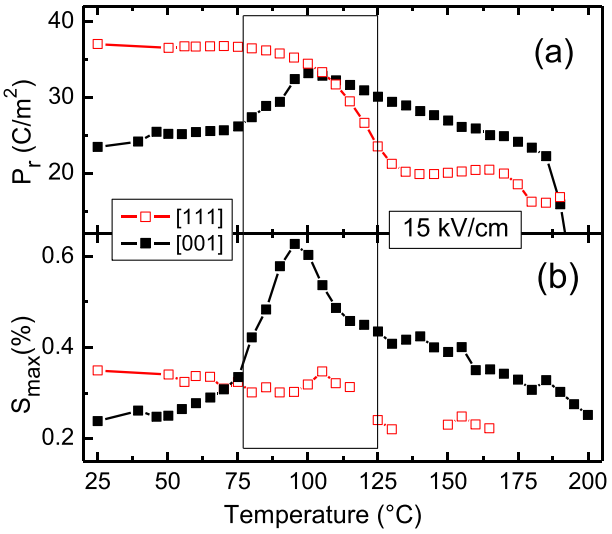

FIG. 2. Temperature dependence of (a) remnant polarization P_r and (b) maximal bipolar (peak-to-peak) strain S_{max} for the [111] and [001] oriented crystals.

The overall dielectric behavior of the studied crystals is similar to the PMN-xPT system with $x \sim 0.3$ (i.e., near its MPB).[17] In the latter system, $x = 0.3$ is generally regarded as the boundary between relaxor and normal ferroelectric behaviour but this boundary is not an abrupt one by any means. For our PIN-PMN-PT SCs, several relaxor characteristics have been observed, such as the dielectric dispersion around T_{max} and the appearance of well-defined phase transitions after poling. Likewise, the inverse dielectric permittivity at 100 kHz (data not shown) shows a deviation from the linear Curie-Weiss law at ~300 °C, which point can be established as the Burns temperature for relaxors.[18] On the other hand, the frequency dependence of T_{max}, one of the most definitive behaviors of relaxors, appears rather weak over the shown frequency range. This could be due to a smearing effect caused by other origins of dielectric relaxation present at low frequencies, e.g., defect dipoles.

Fig. 2(a) shows the measured remnant polarization, P_r, of the [111] and [001] oriented crystals as a function of temperature. Overall, P_r for both crystals shows an anomaly related to T_C as well as a lower temperature anomaly. Comparison with the measured dielectric spectra suggests a difference in the temperature of the intermediate anomaly, especially for the [001] oriented crystal, indicating that the associated transition is E-field dependent.[19,20] (P_r is measured using a cyclic electric field of 15 kV/cm.) On the other hand, the P_r's of the [001] and [111] oriented crystals decrease and increase, respectively, by a similar percentage of ~42% over this transition. This magnitude of change strongly suggests a significant change in the inclination angle between $\boldsymbol{P_s}$ and the two sample orientations.[20] In light of this result, we tentatively attribute a [110] to [001] (i.e., O-T) $\boldsymbol{P_s}$ rotation pathway for the [001] oriented crystal and a [111] to [001] (R-T) $\boldsymbol{P_s}$ rotation pathway for the [111] oriented crystals, respectively (without consideration of possible intermediate M phases). The temperature dependence of the maximal bipolar strain, S_{max}, shows qualitatively similar behavior to that shown by P_r (Fig. 2(b)), e.g., a step-like reduction for the [111] oriented crystal at the

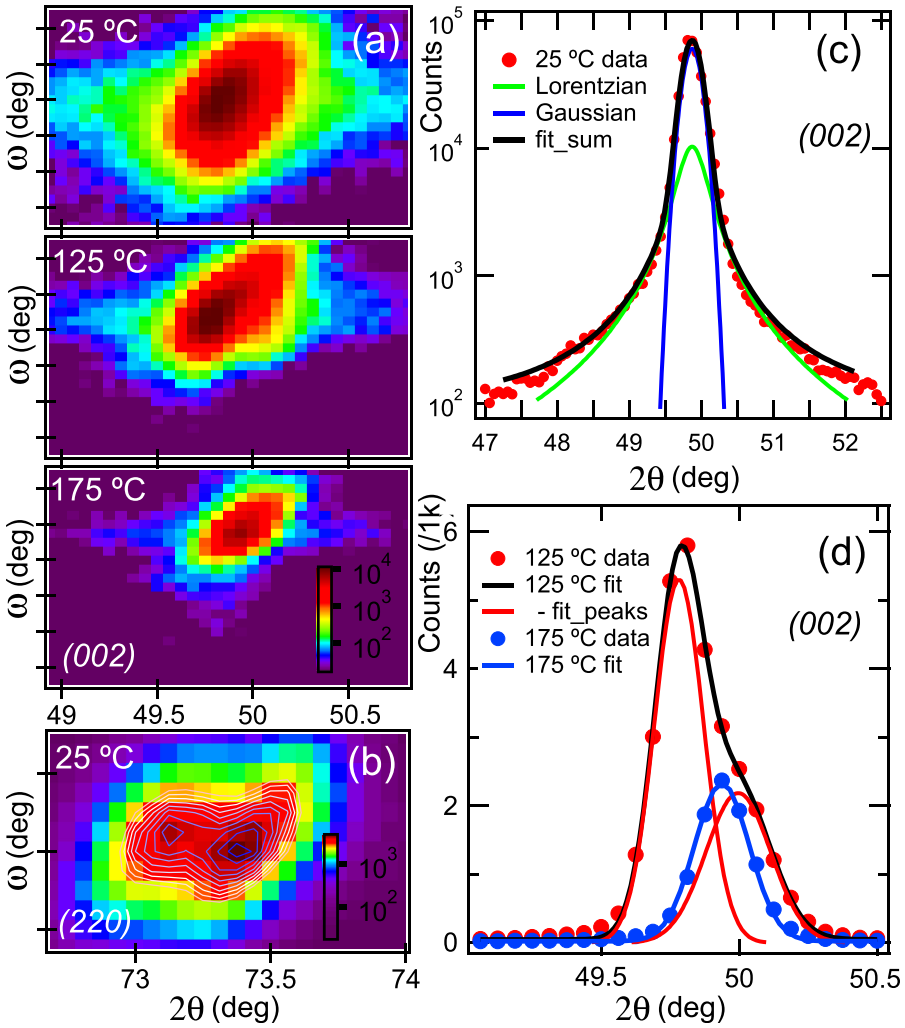

FIG. 3. Selected maps of (a) (002) and (b) (220) reflections for the unpoled crystals. The tick spacing along the ω axes is 0.2°. Intensity contours (2000–4000) are overlaid on (b). (c) and (d) show the ω-integrated 2θ spectra of the (002) reflections at 25 °C and 125/175 °C, respectively, along with their fits.

intermediate temperature transition. In both cases, the observed strain behavior reflects the structure-defined, intrinsic piezoactivity as well as the activity associated with ferroelastic domain switching.

Based on the phase transition sequences deduced from these property studies, diffraction measurements were then taken in each phase region to confirm the metric symmetry of the various structures. Usually, a large number of single domain reflections are collected to determine the metric symmetry of SCs. For ferroelectric SCs, however, there are invariably ferroelastic domains/twins that form in a specific way dependent on the directions of $\boldsymbol{P}_s$ and the applied E fields.[21] The presence of these domain variants adds macroscopic symmetry elements, i.e., pseudo-symmetry, to the crystals (e.g., in the R phase 70.53° and 109.47° domain walls lead to {100} and {110} mirror planes, respectively), and accordingly produce a specific twinned structure in reciprocal space. We thus acquired just five reflections (002/004, 220, 113, 013, and 222) on the *H0L* or *HHL* scattering planes. By using 2θ-ω scanning coupled with the WOMBAT area detector, a volume of reciprocal space was carefully probed around each scanned reflection looking for characteristic peak splittings. This method is in drastic contrast to powder diffraction, in which no twinning information is retained. For ease of the data presentation and analysis, here we reduce the data collected to 2D maps by integrating them along the detector Z-axis, and in some cases, further to 1D ω-integrated spectra.

Fig. 3(a) shows the selected (002) reflection scanned in the *H0L* plane for the unpoled crystals. First, we point out that these profiles contain a clear component of diffuse scattering/streaking that remains even after poling (cf. Fig. 5(a) below), implying an abundance of local structure/s rather than a single well-defined, long range ordered structural state for the studied composition. We attribute this local disorder to the existence of local polar nano regions (PNRs) running along different directions to the dominant polar direction embedded in the crystals. As an example, the ω-integrated spectrum of the (002) reflection at 25 °C is shown in Fig. 3(c). This spectrum can be well fitted to the sum of a Gaussian peak and a Lorentzian peak, corresponding to the Bragg and diffuse scattering components, respectively. From the width of the Lorentzian peak, a correlation length of 20-30 nm is estimated. This length scale is comparable to that observed in the PMN-xPT ($x < 0.3$) system, for example, a correlation length of ~35 nm for $x = 0.2$.[22] The presence of relatively large PNRs is consistent with the weak relaxor characteristics of the crystals as found via dielectric spectroscopy. These large PNRs may indeed play a more essential role than the apparent "monoclinicity" in producing the high

piezoactivity of RF SCs',[22] though the determination of this is not an aim of the current study.

On the other hand, none of the (002) reflections obtained show clear splittings over the temperature range 25 °C–200 °C. At 25 °C, the (220) reflection (see Fig. 3(b); discussed in more detail later) shows a clear 1:1 doublet in 2θ, leading to the assignment of an *R* phase with cell parameters: $a_R = 4.038$ Å; $\alpha = 89.82°$. At 175 °C, a noticeable shift in the 2θ value of the (002) peak confirms a transition to a nonpolar, metrically cubic *C* phase ahead of T_m. This transition is also apparent in the accompanying 3-fold reduction in the intensity of the peak (Fig. 3(d)) due to modified extinction conditions.[7]

The ω width (i.e., the mosaicity) of the (002) peak measures 0.37° at 25 °C, in contrast to the 0.2° ω width of the [001] poled crystal, indicating that the degree of long range ferroelectric order is enhanced by *E*-field poling. This enhancement is attributed to the coalescence and coarsening of the initially fine (typical width ~150 nm), highly disordered micro-domain patterns observed in PFM (piezoresponse force microscopy) images of PIN-PMN-PT SCs.[23] The *R*-*C* transition of the unpoled crystals may involve smeared and localized *T*-like distortions. This is indicated by the appearance of small asymmetries on the broad profile of the (002) reflection at, e.g., 125 °C. As shown in Fig. 3(d), the 2θ spectrum of this reflection is fitted to two peaks centered at $d = 2.021$ Å and 2.014 Å, suggesting a *c*/*a*, *T* distortion of ~1.003. However, the high degree of overlap along ω of these two peaks (cf. Fig. 5(a)) as well as the basically unchanged (220) reflection at 125 °C (not shown) precludes the assignment of a well-defined *T* phase. The absence of any abrupt intermediate symmetry change in the unpoled crystals is consistent with our dielectric data as well as a recent Brillouin spectroscopy study on similar near-MPB PIN-PMN-PT SCs.[24]

Fig. 4(a) shows the (220) reflection scanned in the *HHL* plane at 25 °C for the crystal poled along [111]. The reflection scan shows a clear doublet profile, similar to that for the unpoled crystal (Fig. 3(b)) but with a larger 2θ doublet splitting. At the same temperature, the (004) reflection scanned in the *H0L* plane is not split (Fig. 4(c)). Poling has thus enhanced the extent of the rhombohedral *R* distortion (resulting parameters: $a_R = 4.040$ Å; $\alpha = 89.7°$), rather than changing its symmetry. Note that the (220) doublet is observed at a single ω value (see Fig. 4(a)). It actually corresponds to an out-of-plane (2–20) Bragg peak on the high-2θ side twinned with the in-plane (220) peak about the (100) domain walls; both are captured along the Z-axis on the detector, as illustrated in Fig. 4(b). The presence of such twinned domains means that a 1*R* domain engineered state is not achieved by

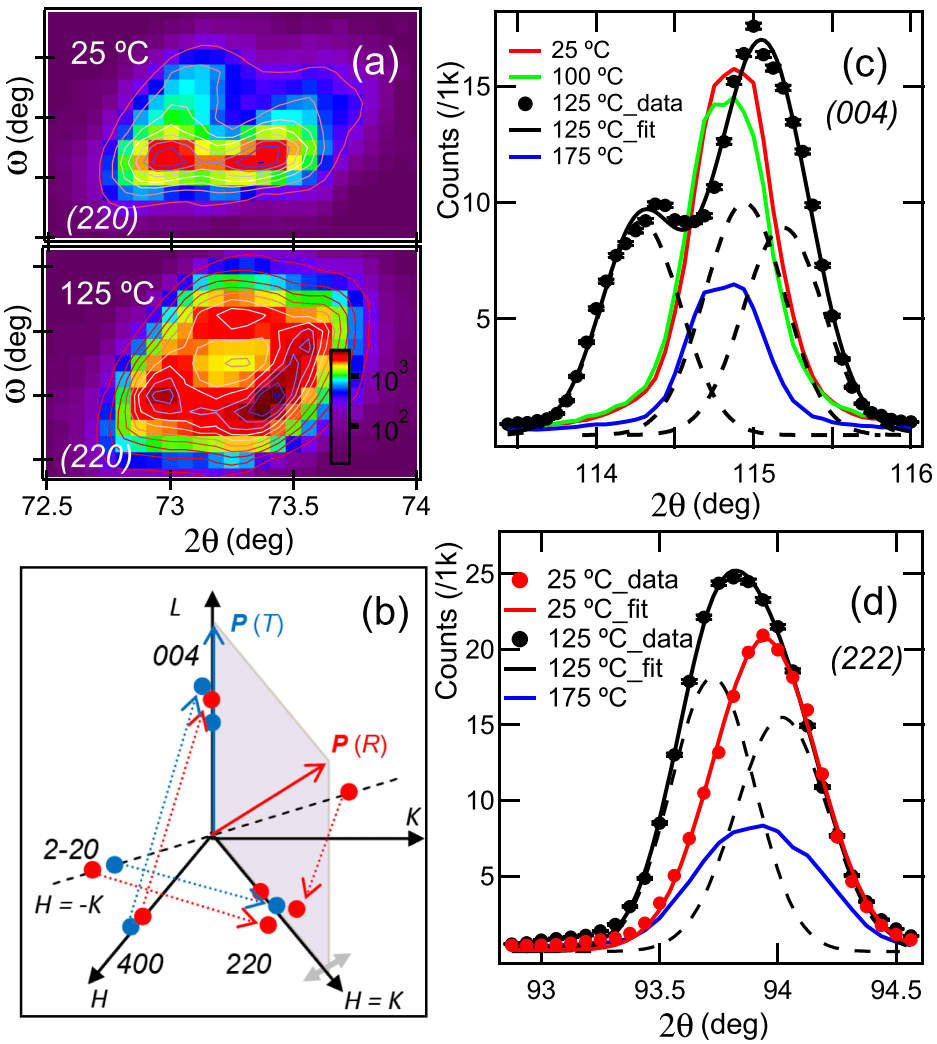

FIG. 4. (a) (220) reflection maps at 25 °C and 125 °C for the [111] poled crystal, with intensity contours (0-3000) overlaid. The tick spacing along the ω axes is 0.2°; (b) Diagram showing the *HHL* scattering plane and accessible {220}/{004} Bragg peaks for *R* (red dots) and *T* (blue dots) phases. The dotted lines represent the twinning relationships in the respective phase. (c) and (d) show the 2θ spectra of the (004) and (222) reflections, respectively, along with their fits. The dashed lines show the decomposed peaks as detailed in the text.

our poling method. Dietze *et al.* reported that a 1*R* state can only be obtained for [111]-oriented PMN-0.29PT SCs via the field-cooling through T_C poling procedure.[14] Note also that monoclinic *M* phases are unlikely to be present as in that case non-equivalent {004} Bragg peaks should be detected.

No noticeable changes are observed in either the (004) or the (220) reflections from 25 °C to 100 °C (not shown), verifying the stability of the *R* phase over this temperature range. At 125 °C, however, the (220) reflection becomes noticeably broader and its overall intensity increases significantly, indicative of an increase in the number of domain variants present. In the scanned profile of the (220) reflection, at least three distinct Bragg peaks are obvious: two of which have the same ω value and are essentially centered at the same 2θ positions as in the prior *R* phase; the new peak corresponds to a *d* spacing of 1.426 Å. We thus infer that *R* and *T* phases coexist at this temperature, a typical behavior associated with first-order phase transitions. In the tetragonal *T* phase, $\boldsymbol{P}_s$ can be oriented along all three $\langle 001 \rangle$ axes in the absence of an applied *E*-field. That is, there should exist 90° twinned domains that split the (004) reflection into a doublet (again with one peak slightly out of the *HHL* plane; see Fig. 4(b)). The decomposed {004} peaks, i.e., $(004)_T/(400)_R/(400)_T$, are shown plotted in Fig. 4(c) (the black dashed lines) in sequence from low to high 2θ. From this decomposition, the lattice parameters of the *T* structure can be extracted as follows: $c_T = 4.052$ Å; $a_T = 4.033$ Å. These parameters also fit well with the d $(= a/2\sqrt{2})$ value for the new (220) peak. The tilt angle between these *T* and *R* domains, calculated using $(\Delta\omega - \Delta 2\theta/2)$ from the observed {220} peaks, is 0.41° in line with the distortion angle $(= 90° - \beta$, β is the angle between the [001] and [110] axes[8]) obtained from the *R* phase. Similarly, the (222) reflection at 125 °C can be decomposed into a $(222)_T$ and a $(222)_R$ peak (see Fig. 4(d)), with *d* spacings of 1.166 Å and 1.163 Å, respectively. Note that the other potential (222) peak ($d = 1.173$ Å at 25 °C) of the *R* phase is absent here, suggesting that the domain variants in the scanned *HHL* plane are fully eliminated after poling so that the $(222)_R$ and $(22\text{-}2)_R$ peaks do not twin with each other. The assumed scenario is thus self-consistent from the diffraction point of view. It is also noted that the $(2\text{-}20)_R$ peak is elongated along ω and toward high 2θ angle. This may be due to internal tensile stresses arising from the domain reconfiguration process. On further heating, the crystal undergoes depolarization at a temperature below 175 °C, as verified by the *C* phase (004) and (222) peaks (Figs. 4(c) and 4(d)), though no diffraction data were surveyed in the stability field of the *T* phase.

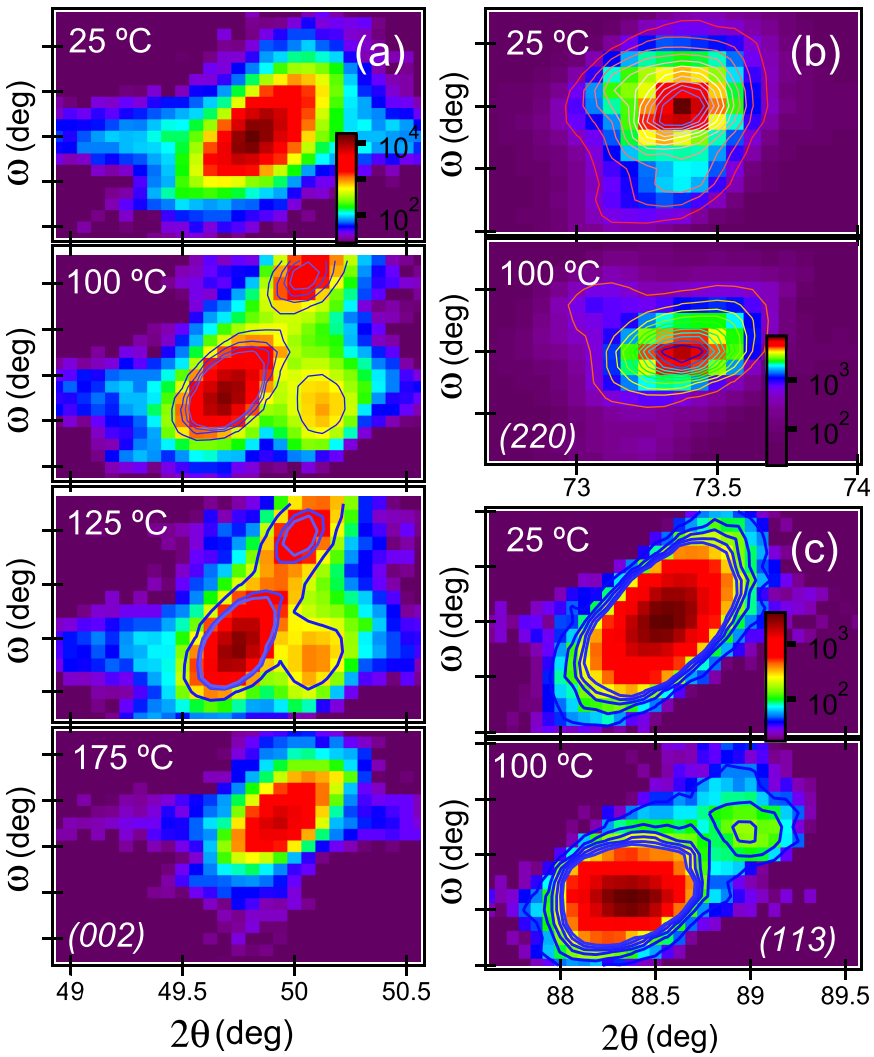

FIG. 5. Selected maps of (002) (a), (220) (b), and (113) (c) reflections for the [001] poled crystal. The overlaid intensity contours are 0-2000 in (a), 0-5500 in (b), and 0-3000 in (c). The tick spacing in ω axes is 0.2°.

Fig. 5 shows profiles of the (002) and (220) reflections for the poled [001] crystal scanned in the *H0L* and *HHL* planes, respectively. At 25 °C, the (002) reflection shows no splitting, expected as poling along [001] can induce a four-variant domain engineered state, regardless of the symmetry (either R/M_A or O/M_C here).[21] On the other hand, the (220) reflection appears to consist of a major peak with a shoulder having rather close ω but no split 2θ positions (cf. Figs. 3(b) and 4(a)); in this case, the (220) and (2-20) peaks have the same d value and overlap with each other in reciprocal space after twinning about the (100) and (110) planes. This implies that $\boldsymbol{P_s}$ is confined to the (100) lattice plane, thus effectively ruling out potential R/M_A structures. Consistent reciprocal space profiles of the (002)/(220) reflections have been shown by some authors for M_C symmetry.[6–8] The non-validity of an R/M_A phase is also supported by the (113) reflections scanned in the same *HHL* plane. Under the assumption of a $4R/M_A$ domain structure, a twinned (113)/(11-3) reflection (about the (110) plane) should be present, opposite to the actual observation (Fig. 5(c)). As O is a limiting case of M_C when $c_M = a_M$, to distinguish and parameterize them requires a careful comparison of c_M and a_M values. Unfortunately, we lack information on the (200) reflection in the present case. As an alternative method, we refined five scanned reflections using DICVOL04 software.[25] These five peaks themselves cannot adequately establish the true lattice as several plausible indexing solutions yielded high figure-of-merits (FOM). Nevertheless, one of these indexing results, an O lattice with $a_O = 5.699$ Å, $b_O = 5.728$ Å, and $c_O = 4.006$ Å (FOM: M(5) = 212), conforms to the known base-centered O symmetry and appears most reasonable. This corresponds to an M_C primitive cell with $c_M = a_M = 4.040$ Å, $b_M = 4.006$ Å, and $\beta = 90.29°$.[4]

The O/M_C symmetry found in the as-poled state verifies the $\boldsymbol{P_s}$ rotation pathway inferred from the evolution of the measured P_r. On heating, the $\boldsymbol{P_s}$ is expected to move towards the [001] axis and a true M_C phase ($c_M \neq a_M$) will occur. At 100 °C, the (002) reflection is split into two major peaks, along with a rather weaker one that could lie out of the *H0L* plane. Meanwhile, the (220) reflection also develops a shoulder on the high-d side while the (113) reflection is more clearly shifted and splits into new peaks centered at $d = 1.214$ Å and 1.221 Å, due to the occurrence of 90° domain walls. It is found that a single tetragonal T structure with $c_T = 4.051$ Å and $a_T = 4.022$ Å best fits all the measured 2θ values. The calculated tilting angle ($2\arctan(c/a) - 90°$), using a 90°-domain model, agrees with that measured (~0.36°) from the $(002)_T/(200)_T$ peaks. The observation of a T phase at this temperature, however, apparently contradicts the dielectric spectra obtained on the same crystal. We speculate that this may be due to a "memory effect," i.e., a poling history dependence of the M_C-T transition, similar to the case reported by Shen and Cao on PZN-0.08PT SCs.[26] Moreover, no abrupt changes are seen in the diffraction data at 125 °C except that the T phase has a decreased c/a ratio of 1.005, and again the crystal is in a C phase by 175 °C (see Fig. 5(a)).

IV. SUMMARY

In summary, the crystal structure of 0.26PIN-0.46PMN-0.28PT SCs has been studied by means of neutron diffraction coupled with dielectric, pyroelectric, and ferroelectric measurements. The crystals show several typical relaxor dielectric behaviors, including the observation of PNR-associated diffuse scattering. The unpoled crystal apparently has an average R symmetry throughout its ferroelectric phase stability field. E-field poling along [111] enhances the R distortion and induces a first-order R-T transition near 125 °C. After poling along [001], the crystal has an O/M_C ground state and then undergoes an M_C-T-C transition sequence on increasing the temperature. Finally, we comment that the structural behavior of the PIN-PMN-PT system appears highly analogous to that of its binary precursor, PMN-PT with very close PT content, as judged by a comparison of our results with those made on the latter system.

ACKNOWLEDGMENTS

Q.L., Y.L., and R.L.W. acknowledge the support of the Australian Research Council (ARC) in the form of ARC Discovery Grants. Y.L. also acknowledges support from the ARC Future Fellowships Program.

[1]S.-E. Park and T. R. Shrout, J. Appl. Phys. **82**, 1804 (1997).
[2]X. Li and H. Luo, J. Am. Ceram. Soc. **93**, 2915 (2010).
[3]S. Zhang and F. Li, J. Appl. Phys. **111**, 031301 (2012).
[4]B. Noheda, D. E. Cox, G. Shirane, S.-E. Park, L. E. Cross, and Z. Zhong, Phys. Rev. Lett. **86**, 3891 (2001).
[5]D. E. Cox, B. Noheda, G. Shirane, Y. Uesu, K. Fujishiro, and Y. Yamada, Appl. Phys. Lett. **79**, 400 (2001).
[6]Z.-G. Ye, B. Noheda, M. Dong, D. Cox, and G. Shirane, Phys. Rev. B **64**, 184114 (2001).
[7]K. Ohwada, K. Hirota, P. W. Rehrig, Y. Fujii, and G. Shirane, Phys. Rev. B **67**, 094111 (2003).
[8]F. Bai, N. Wang, J. Li, D. Viehland, P. M. Gehring, G. Xu, and G. Shirane, J. Appl. Phys. **96**, 1620 (2004).
[9]H. Fu and R. E. Cohen, Nature **403**, 281 (2000).
[10]Y. M. Jin, Y. U. Wang, A. G. Khachaturyan, J. F. Li, and D. Viehland, Phys. Rev. Lett. **91**, 197601 (2003).
[11]W. S. Chang, L. C. Lim, P. Yang, H. Miao, C.-S. Tu, Q. Chen, and A. K. Soh, Appl. Phys. Lett. **94**, 202907 (2009).
[12]Q. Li, Y. Liu, V. Luzin, A. J. Studer, Y. Wan, Z. Li, L. Norén, R. L. Withers, and Z. Xu, J. Appl. Phys. **111**, 084110 (2012).
[13]W. D. Dong, P. Finkel, A. Amin, and C. S. Lynch, Appl. Phys. Lett. **100**, 262909 (2012).
[14]M. Dietze, H. Katzke, M. Es-Souni, N. Neumann, and H. Luo, Appl. Phys. Lett. **100**, 242905 (2012).
[15]A. J. Studer, M. E. Hagen, and T. J. Noakes, Physica B **385**, 1013 (2006).
[16]Z. Li, Z. Xu, X. Yao, and Z.-Y. Cheng, J. Appl. Phys. **104**, 024112 (2008).
[17]E. V. Colla, N. K. Yushin, and D. Viehland, J. Appl. Phys. **83**, 3298 (1998).
[18]A. A. Bokov and Z.–G. Ye, J. Mater. Sci. **41**, 31 (2006).
[19]M. Davis, D. Damjanovic, and N. Setter, Phys. Rev. B **73**, 014115 (2006).
[20]A. Herklotz, J. D. Plumhof, A. Rastelli, O. G. Schmidt, L. Schultz, and K. Dörr, J. Appl. Phys. **108**, 094101 (2010).
[21]M. Davis, D. Damjanovic, D. Hayem, and N. Setter, J. Appl. Phys. **98**, 014102 (2005).
[22]P. M. Gehring, J. Adv. Dielectr. **2**, 1241005 (2012).
[23]Q. Li, Y. Liu, R. L. Withers, Y. Wan, Z. Li, and Z. Xu, J. Appl. Phys. **112**, 052006 (2012).
[24]T. H. Kim, S. Kojima, and J. Ko, J. Appl. Phys. **111**, 054103 (2012).
[25]A. Boultif and D. Louer, J. Appl. Crystallogr. **37**, 724 (2004).
[26]M. Shen and W. Cao, Appl. Phys. Lett. **86**, 192909 (2005).